

# The effects of crystallite growth and dopant migration on the carbon monoxide sensing characteristics of nanocrystalline tin oxide based sensor materials

Steven R. Davis, Alan V. Chadwick and John D. Wright\*†

Centre for Materials Research, School of Physical Sciences, University of Kent, Canterbury, Kent, UK CT2 7NR

Tin oxide nanocrystals, both pure and  $\text{Cu}^{2+}$  and  $\text{Fe}^{3+}$  doped, have been prepared by a sol-gel process. The response of these materials to carbon monoxide in dry air has been investigated as a function of annealing temperature. The growth of the crystallites was monitored by XRPD from room temperature to about  $900^\circ\text{C}$  and the response of the material to CO was studied for materials annealed over that temperature range. All of the materials were shown to respond to low concentrations of CO with a narrow peak in sensitivity at an operating temperature of about  $200^\circ\text{C}$ . A good response to CO was also observed at an operating temperature of about  $400^\circ\text{C}$ . No improvements in selectivity to CO were observed by the addition of either of the cation dopants. The sensitivity to CO was shown to decrease as crystallite size increased. The addition of the metal cation dopants impeded crystallite growth. Our previously reported Cu K-edge and Fe K-edge EXAFS measurements, on the  $\text{Cu}^{2+}$  and  $\text{Fe}^{3+}$  doped materials respectively, showed the dopant cations to move from ordered  $\text{Sn}^{4+}$  substitutional lattice sites in the as-prepared materials to more disordered regions, most likely the surface regions, as the materials were annealed. This dopant migration begins at about  $400^\circ\text{C}$  and is accompanied by a corresponding large decrease in response to CO at an operating temperature of about  $200^\circ\text{C}$  (the peak in sensitivity). This is attributed to the migration of the dopants to the surface of the crystallites and speculative explanations are given. The reduction in response of the same materials at an operating temperature of about  $400^\circ\text{C}$  is not so large, indicating the response mechanisms at 200 and  $400^\circ\text{C}$  to be different.

The detection of flammable gases and vapours in air is a matter of considerable current interest and importance. In addition to the obvious dangers associated with the flammable nature of these gases and vapours, many of them are also harmful at very low concentrations, where their presence is undetectable by the human senses.

Metal oxides, in particular tin oxide, have been widely employed as the active element in flammable gas sensors.<sup>1-3</sup> Recently, the use of nanocrystalline tin oxide (with average crystallite sizes of less than 10 nm) has become more common since sensitivity has been shown to vary inversely with crystallite size.<sup>4,5</sup> Such devices are capable of detecting low ppm and even ppb concentrations of flammable gas in dry air<sup>6</sup> but an inherent problem remains their lack of selectivity. Considerable research has been conducted into improving the selectivity of these devices by the incorporation of noble metal catalysts,<sup>7,8</sup> the addition of metal cation dopants<sup>9</sup> and the preparation of novel ternary compounds.<sup>10,11</sup> Whilst many improvements in selectivity are often reported, there is little understanding of the reasons for this. A hindrance to the development of improved tin oxide based gas sensors is the dependence of the gas sensing properties on the preparation method used for material of a given chemical composition. Different preparation methods and deposition techniques affect not only the porosity but also the defect structure of the oxide modifying the semiconductivity and hence the response characteristics. The thickness of the gas sensing layer,<sup>12</sup> the positioning of the electrodes<sup>2</sup> and the nature of the electrode material<sup>13</sup> are other parameters known to influence the final characteristics of the sensors. Several routes exist to nanocrystalline  $\text{SnO}_2$  including sol-gel synthesis<sup>14,15</sup> and vacuum sputtering<sup>16,17</sup> and these have all been used to produce materials with improved catalytic and sensing performance. The sol-gel route offers a simple

method of incorporating dopants into the material and enhancing the selectivity of  $\text{SnO}_2$  in both catalytic and sensing applications. For example, doping  $\text{SnO}_2$  with  $\text{Cu}^{2+}$  cations promotes the oxidation of carbon monoxide by oxygen or nitric oxide.<sup>18,19</sup> A wide variety of cationic dopants have been used to improve the selectivity of  $\text{SnO}_2$  gas sensors and it is worth noting that  $\text{Cu}^{2+}$  doping has also been claimed to enhance the detection of hydrogen sulfide.<sup>20</sup>

We have been investigating the use of both metal cation doped and catalyst modified nanocrystalline tin oxide materials for applications in environmental monitoring. This type of application requires the sensor materials to possess both high sensitivity, since most occupational exposure standards are typically less than 50 ppm, and good selectivity as well as a short response time. Selectivity is an important requirement since different flammable gases and vapours can have widely differing exposure standards and some will therefore present a greater risk to health at low concentrations whereas others may be relatively harmless in the short term at that same concentration. A short response time is important if these devices are to act as an early warning of danger.

Recently, we reported on a combined extended X-ray absorption fine structure (EXAFS) and X-ray powder diffraction (XRPD) study of both pure and  $\text{Cu}^{2+}$  and  $\text{Fe}^{3+}$  cation doped nanocrystalline tin oxide.<sup>21</sup> These materials were prepared *via* a sol-gel route and the study showed that the as-prepared materials possess an average crystallite size of 2–3 nm. The incorporation of the dopants did not affect the crystallite size. Cu K-edge and Fe K-edge EXAFS of the doped materials showed that the dopant cations were located on Sn substitutional sites in both materials in their as-prepared state. All of the materials were subjected to thermal annealing, resulting in crystallite growth as measured from the XRPD patterns. The incorporation of the dopants hindered crystallite growth in agreement with other studies.<sup>4,5</sup> The EXAFS measurements on the dopant edges in both materials showed that at tempera-

†E-mail: J.D.Wright@ukc.ac.uk

tures above about 400 °C, the dopants migrate from ordered substitutional sites within the lattice to more disordered regions, most likely the surface regions of the nanocrystals. This was supported by comparison with EXAFS data for deliberately prepared surface doped materials. Tin oxide gas sensors are typically run at elevated temperatures and in the present study we report on the effects that the increases in average crystallite size and the migration of added cation dopants have on the response of the semiconductivity of these materials to carbon monoxide.

## Experimental

### Materials preparation

The preparation followed the method of Ansari *et al.*<sup>15</sup> A 0.1 M solution of tin chloride pentahydrate (Aldrich, 98% purity) was prepared by dissolving 1.402 g in 40 ml of distilled water. To this solution 5 ml of aqueous ammonia (0.880 w/w, Fisons) were added and the solid from the resulting gel was recovered by evaporation of the water in an oven at 100 °C. The ammonium chloride by-product was removed by extensive washing with distilled water. The washed material was dried in an oven at 100 °C overnight and ground using an agate mortar and pestle. The X-ray powder diffraction pattern confirmed the material was nanocrystalline tin oxide.

Cationic dopants were introduced by adding the appropriate amount of the metal chloride (CuCl<sub>2</sub> and FeCl<sub>3</sub>) to the initial tin chloride solution and following the above procedure. Samples were prepared with nominal dopant concentrations of 1, 5 and 10 mol% for copper and iron.

For comparative purposes samples of the pure nanocrystalline SnO<sub>2</sub> were surface coated with Cu<sup>2+</sup> and Fe<sup>3+</sup> cations. CuCl<sub>2</sub> and FeCl<sub>3</sub> aqueous solutions were prepared by dissolving the appropriate amount of metal salt in 5 ml of distilled water in a 10 ml beaker. The as-prepared nanocrystalline tin oxide was added and the mixture stirred whilst allowing the water to evaporate leaving coated samples. Tin oxide samples were prepared coated with nominal 1 and 5 mol% Cu<sup>2+</sup> and Fe<sup>3+</sup> cations with respect to the total number of Sn<sup>4+</sup> cations (both bulk and surface). These samples were assumed to be surface doped, as in previous studies.<sup>22</sup>

### Laboratory XRPD and combined EXAFS/XRPD

X-Ray powder diffraction patterns of all the samples were collected using a Phillips PW1050 powder diffractometer. Crystallite sizes, *S*, were determined from the Debye–Scherrer equation,<sup>23</sup> *i.e.*

$$S = \frac{K\lambda}{\beta \cos \theta}$$

where *K* is a constant (0.89),  $\beta$  is the full-width-at-half-maximum-height of a diffraction peak at angle  $\theta$ , and  $\lambda$  is the X-ray wavelength (in the present work Cu-K $\alpha$  radiation was employed).

Combined EXAFS/XRPD measurements were made on station 9.3 at the CLRC Daresbury Synchrotron Radiation Source, the details of which have been previously reported.<sup>21</sup>

### Sensor fabrication

Sensors were fabricated by applying a thin layer of the SnO<sub>2</sub> material to a standard Rosemount substrate (these are no longer in production—a similar design is available from Capteur Sensors Ltd, 66 Milton Park, Abingdon, Oxon, OX14 4RY, UK). The substrates are made from alumina with platinum interdigitated electrodes on one side and a platinum heater on the obverse side. The SnO<sub>2</sub> was applied to the substrate using a glass pipette from a thick suspension in ethanol. The sensor material was then ‘initialised’ by heating

it to *ca.* 400 °C on the substrate itself in clean, dry air. This initialisation procedure was found to be necessary to obtain reproducible responses to CO.

### CO gas sensing measurements

The sensors were tested using a fully computer-controlled gas sensor test rig as developed by Archer *et al.*, the details of which have been described elsewhere.<sup>24</sup> CO was supplied by BOC Special Gases (1% CO in air and 22.0 ppm CO in air certified) and this was diluted with clean, dry air as necessary to provide a wide range of pollutant gas concentrations. The air was filtered and then dried using a Pneumatic Products air dryer (model P3HA-E3-40). The conductance of the sensors was measured every 5 s. Two main types of gas sensing measurements were made with each of the sensor materials. Firstly, a temperature profile of sensitivity was obtained to identify the temperature of maximum response to CO by exposing the sensors to fixed concentrations of CO at varying operating temperatures. The gas sensor test-rig allows the sensors to be operated at sixteen discrete temperatures (from room temperature to about 420 °C). Secondly, sensor calibrations were performed by exposing the sensors to varying concentrations of CO at fixed temperatures. For both types of experiment, the sensors were typically exposed to 120 s pulses of CO followed by 120 s reversal in clean, dry air and the percentage response determined by:

$$\text{Response (\%)} = \frac{G_{\text{gas}} - G_{\text{air}}}{G_{\text{air}}} \times 100$$

where  $G_{\text{gas}}$  is the conductance of the sensor in CO and  $G_{\text{air}}$  is the conductance in dry air.

## Results

The as-prepared materials have an average crystallite size of between 2 and 3 nm, as determined from the XRPD patterns. Transmission electron micrographs confirmed the nanocrystalline nature of the samples and showed the crystallites to be agglomerating, but were of too low resolution for accurate size determination. The incorporation of either the Cu<sup>2+</sup> or Fe<sup>3+</sup> cations had no effect on the average crystallite size prior to annealing. Fig. 1 shows the effect of annealing on the average crystallite size for both the pure and doped tin oxide materials. The data were obtained by heating each of the materials at a rate of 5 °C min<sup>-1</sup> and taking the XRPD pattern approximately every 5 min from which the average crystallite sizes were deduced. Full details of this process have previously been given.<sup>21</sup> It is apparent that the addition of both dopants

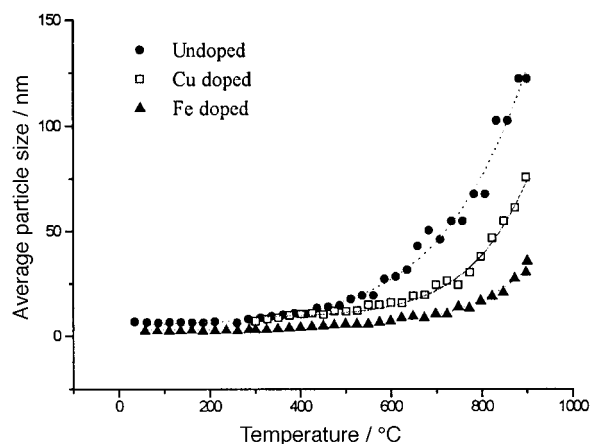


Fig. 1 The dependence of particle size of various tin oxide samples during heating at 5 °C min<sup>-1</sup>; (●) pure tin oxide, (□) nominal 5 mol% Cu<sup>2+</sup>, (▲) nominal 5 mol% Fe<sup>3+</sup>

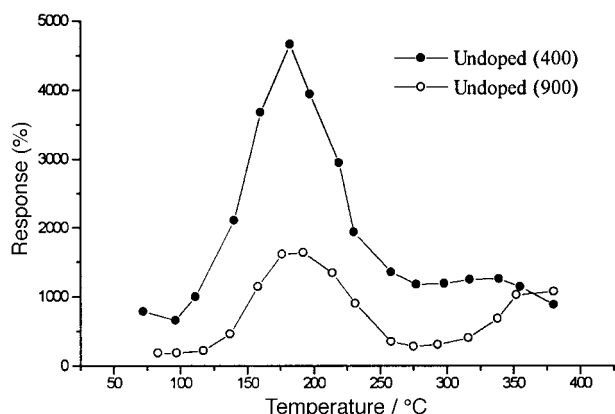


Fig. 2 Temperature profiles of sensitivity of undoped sol-gel prepared tin oxide sensors annealed at 400 °C (●) and 900 °C (○) overnight

impedes the crystallite growth. This is particularly marked in the case of  $\text{Fe}^{3+}$  and is in agreement with previous studies.<sup>5</sup>

### Response of $\text{SnO}_2$ to CO

Fig. 2 shows the temperature profiles of sensitivity for two pure tin oxide sensors to 800 ppm CO in dry air. The material for the first sensor (filled circles) was annealed at 400 °C (standard initialisation procedure) for 1 h whereas the other (open circles) was annealed at 900 °C for 1 h in a furnace prior to application to the substrate. The shape of both of the profiles is identical, peaking in sensitivity to CO at just less than 200 °C. However, the magnitude of response of the sensor annealed at 900 °C is much less than that of the sensor annealed at 400 °C. This can only be attributed to the increase in average crystallite size, which can be seen from Fig. 1 to be increased from about 10 nm at 400 °C to over 100 nm at 900 °C. Interestingly, there is no difference in the magnitudes of response of the two sensors at the highest operating temperature (just less than 400 °C). Fig. 3 shows the variation of sensor current as a function of time as both sensors were exposed to 120 s pulses of air/gas/air at each of the available operating temperatures. This is the raw data used to determine the responses shown in Fig. 2. Approximate temperatures have been added to the figure to aid in the discussion although it should be noted that the increase in temperature is not constant with time since the gas sensor test-rig is only capable of delivering sixteen discrete temperatures. This figure and the

corresponding temperature profile shown in Fig. 2 highlight a major flaw in the definition of sensitivity. From Fig. 3, it would appear that the best response to CO is attained at the highest operating temperatures but this is shown in Fig. 2 to be not the case. This is due to the increasing baseline conductance as the operating temperature is increased and is difficult to avoid. In this study, the shapes of the profiles are the major consideration so this does not present a significant problem but has to be borne in mind when comparing the magnitudes of response for the materials possessing differently charged cation dopants. However, Fig. 3 shows that the conductivities of the two samples in clean air are very similar, whereas those in CO differ much more markedly around 200 °C, confirming that at this temperature the change in sensitivity is indeed related to surface chemical processes and hence dependent on surface area.

For both sensors operating at 200 °C (the peak in sensitivity), the speed of the response and reversal is fast with the sensor current reaching its maximum and minimum values respectively during the 120 s pulse lengths. At the higher temperatures, above about 300 °C, this is not the case and the response is incomplete in 120 s (though the reversal is still fast). This is a second factor reducing the apparent sensitivity at high temperatures. Two calibrations were performed in CO over concentration ranges of 2–11 ppm and 1000–3000 ppm at *ca.* 200 °C (the peak in sensitivity) and *ca.* 380 °C with pulse lengths of 120 s and the calibration data are shown plotted in Fig. 4 and 5, respectively. The 400 °C annealed material, in particular, yields very promising results with the relationship between  $\ln[\text{CO}]$  and  $\ln(\text{response})$  being linear over the entire concentration range. This shows the response to follow a power-law dependence on the concentration:

$$\text{Response} = k[\text{CO}]^\beta$$

where  $k$  is the intercept of the  $\ln$ – $\ln$  plot and  $\beta$  is the gradient. From Fig. 4,  $k=3.29$  and  $\beta=0.72$  for the 400 °C annealed material operating at *ca.* 200 °C and  $k=2.30$  and  $\beta=0.68$  for the 900 °C annealed material operating at the same temperature. In effect, the calibration lines are almost parallel and this suggests the mechanism of response for both of the materials to be the same. The 900 °C annealed material appears to begin to saturate within the concentration range considered, evident as a levelling off of the calibration plot, whereas the 400 °C material does not. This can be attributed to the reduction in surface area as a result of sintering.

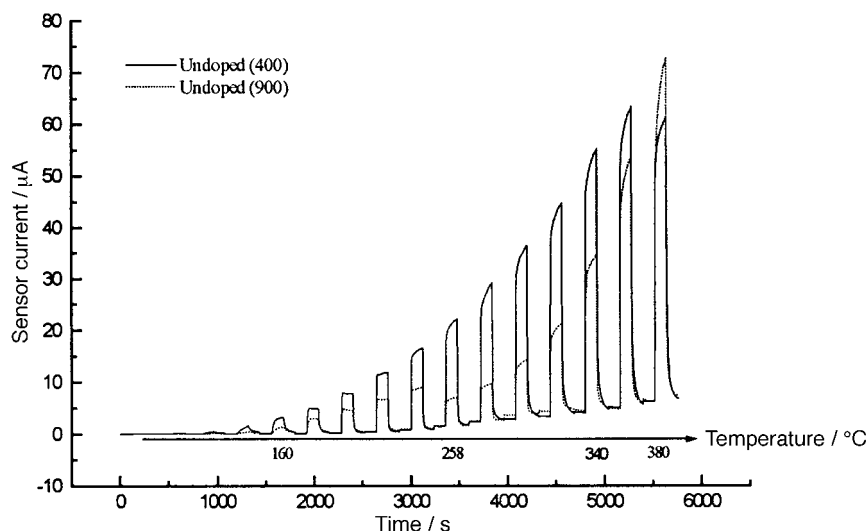
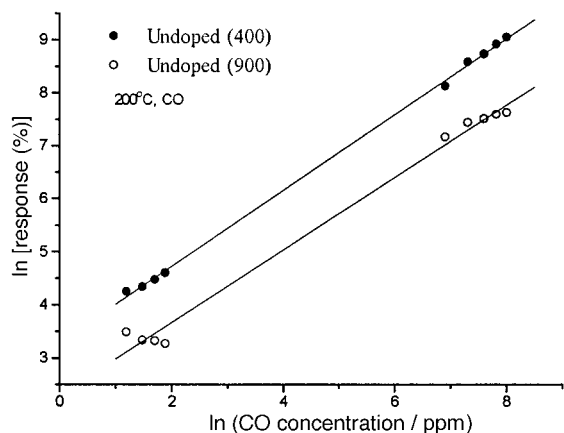
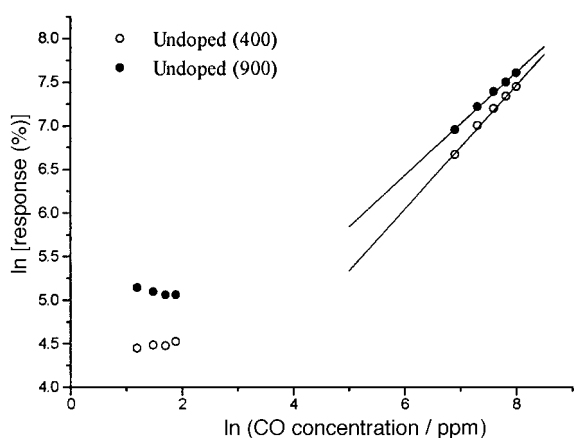


Fig. 3 Variation of sensor current of undoped tin oxide sensors annealed at 400 °C (—) and 900 °C (···) overnight as a function of increasing sensor operating temperature. The sensors were exposed to equal 120 s pulses of dry air followed by CO and followed by dry air again.



**Fig. 4** Calibration data for undoped  $\text{SnO}_2$  sensors annealed at  $400^\circ\text{C}$  (●) and  $900^\circ\text{C}$  (○) overnight to a wide range of CO concentrations in dry air at an operating temperature of *ca.*  $200^\circ\text{C}$ , *i.e.* the peak in sensitivity. The duration of each gas and reversal pulse was 120 s.



**Fig. 5** Calibration data for undoped  $\text{SnO}_2$  sensors annealed at  $400^\circ\text{C}$  (●) and  $900^\circ\text{C}$  (○) overnight to a wide range of CO concentrations in dry air at an operating temperature of *ca.*  $380^\circ\text{C}$ . The duration of each gas and reversal pulse was 120 s for the calibration.

For the same sensors operating at *ca.*  $380^\circ\text{C}$ , a linear relationship is not obtained over the entire concentration range as can be seen from Fig. 5 and instead consists of two linear regions of differing slopes. Although it is possible to fit the data to an exponential growth function, no further manipulation of this function was found to yield a straight line relationship. However, the high concentration data can be fitted to a linear regression and  $\beta$  values of 0.70 and 0.60 are obtained for the  $400^\circ\text{C}$  annealed and  $900^\circ\text{C}$  annealed materials respectively. For both materials, the variation in response to the low concentrations of CO at this high operating temperature is only slight and the data were very noisy in this range. The magnitude of response to the higher concentrations of CO is very similar for both sensors as would be expected from Fig. 2.

#### Response of $\text{Cu}^{2+}$ and $\text{Fe}^{3+}$ doped $\text{SnO}_2$ to CO

Samples of  $\text{SnO}_2$  were prepared doped with nominal 1, 5 and 10 mol%  $\text{Cu}^{2+}$  and  $\text{Fe}^{3+}$  and their response to CO examined. The dopant concentration had no obvious effect on the response characteristics of the sensors and results for just one of these, the 5 mol% doped material, will be presented. The temperature profiles of sensitivity shown in Fig. 6 both have the same peak at *ca.*  $200^\circ\text{C}$  as that observed (Fig. 2) for the undoped material. Hence, since selectivity in tin-oxide-based

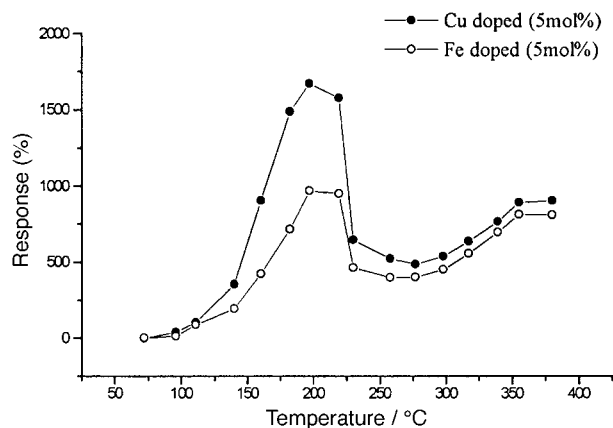


**Fig. 6** Temperature profiles of sensitivity for  $\text{Cu}^{2+}$  (●) and  $\text{Fe}^{3+}$  (○) doped  $\text{SnO}_2$  sensors (both nominal 5 mol%) in 800 ppm CO in dry air. The data were obtained by exposing the sensors to 120 s cycles of air/gas/air at each operating temperature.

sensors is linked to the sharpness and position of peaks in temperature profiles of sensitivity, neither of the doped sensor materials exhibits any enhanced selectivity towards CO. The differing conductance in clean dry air of the two materials as a result of the doping with differently charged cations makes any comparison between the magnitudes of response meaningless as previously mentioned. The reduction in response upon annealing of the undoped  $\text{SnO}_2$  has already been described (Fig. 2) and the same study was performed on both the  $\text{Cu}^{2+}$  and  $\text{Fe}^{3+}$  doped materials. Large batches of both doped materials were made and portions of these materials were pelleted and subjected to 1 h anneals at a range of different fixed temperatures and their responses to CO tested. Sensors were all fabricated in the same manner and underwent the usual initialisation process prior to making the measurements. Fig. 7 shows the change in the temperature profile of sensitivity to 800 ppm CO as the  $\text{Cu}^{2+}$  doped material is annealed at different temperatures. The main feature of this plot is the large reduction in the peak of response at about  $200^\circ\text{C}$ . The response at the highest temperature (about  $400^\circ\text{C}$ ) is also seen to decrease but not quite so rapidly as the low temperature response. Comparison with Fig. 2 shows that the reduction in response at the low operating temperature is far more dramatic

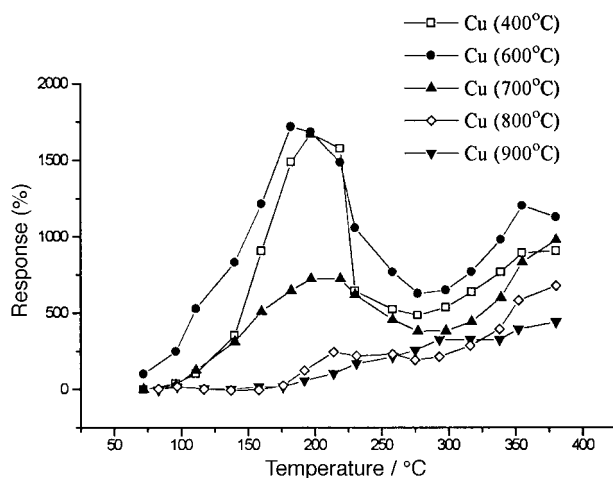


**Fig. 7** Change in temperature profile of sensitivity to 800 ppm CO in dry air for the nominal 5 mol%  $\text{Cu}^{2+}$  doped  $\text{SnO}_2$  as a function of annealing temperature. The samples were prepared by subjecting portions of the same batch of Cu doped  $\text{SnO}_2$  to 1 h anneals at different temperatures. The data were obtained by subjecting the sensors to 120 s cycles of air/gas/air at each of the available operating temperatures.

for the doped material than the undoped. The  $\text{Cu}^{2+}$  doped  $\text{SnO}_2$  sensor was calibrated over a wide range of CO concentrations at operating temperatures of *ca.* 200 and 380 °C and the data are shown in Fig. 8 and 9, respectively. As for the undoped  $\text{SnO}_2$ , the  $\ln(\text{response})$  appears to vary linearly with  $\ln(\text{CO concentration})$  over the wide range considered at the operating temperature of *ca.* 200 °C and also this time at the higher operating temperature. Consider first the sensors operating at the lower temperature (*ca.* 200 °C). From Fig. 8, values of  $k=2.21$  and  $\beta=0.72$  for the 400 °C annealed material and  $k=2.34$  and  $\beta=0.39$  for the 900 °C annealed material are obtained. At the higher operating temperature (*ca.* 380 °C), values of  $k=3.66$  and  $\beta=0.50$  and  $k=3.15$  and  $\beta=0.51$  are obtained for the 400 and 900 °C annealed materials, respectively.

The  $\text{Fe}^{3+}$  doped material was treated in the same way and Fig. 10 shows the change in the temperature profile to 800 ppm CO for this material as a function of annealing temperature. The figure shows all of the same features as observed for the  $\text{Cu}^{2+}$  doped  $\text{SnO}_2$  sensors, *i.e.* the large reduction in response at the operating temperature of about 200 °C. However, for the  $\text{Fe}^{3+}$  doped material, the reduction in the response at this temperature is far more rapid and by 600 °C almost no response

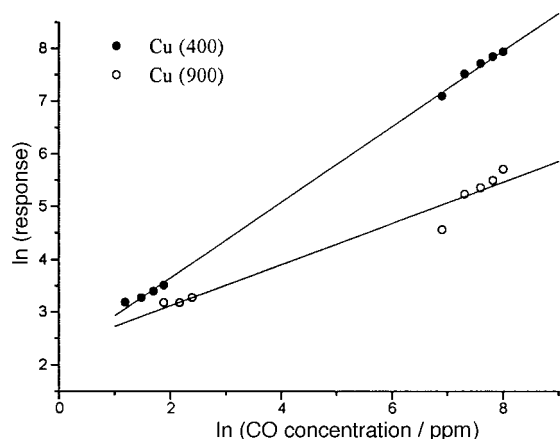


**Fig. 8** Calibration of nominal 5 mol%  $\text{Cu}^{2+}$  doped  $\text{SnO}_2$  sensor at an operating temperature of *ca.* 200 °C in CO in dry air over a concentration range of 3–3000 ppm. The two materials were prepared by subjecting portions of the same batch of  $\text{Cu}^{2+}$  doped  $\text{SnO}_2$  to 1 h anneals at 400 and 900 °C in a furnace. The length of each gas and reversal pulse was 120 s for the calibration.

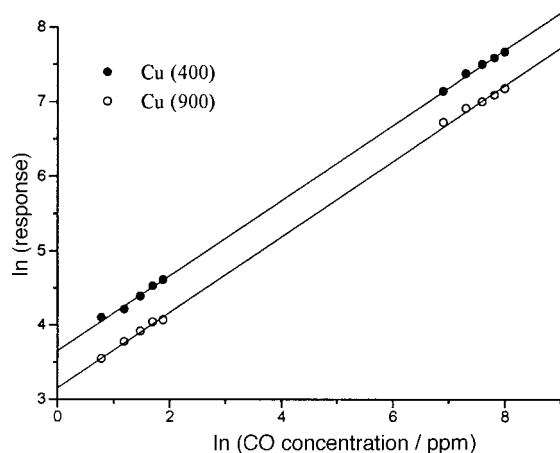


**Fig. 9** Calibration of nominal 5 mol%  $\text{Cu}^{2+}$  doped  $\text{SnO}_2$  sensor at an operating temperature of about 380 °C in CO in dry air over a concentration range of 3–3000 ppm. The two materials were prepared by subjecting portions of the same batch of  $\text{Cu}^{2+}$  doped  $\text{SnO}_2$  to 1 h anneals at 400 and 900 °C. The length of each gas and reversal pulse was 120 s for the calibration.

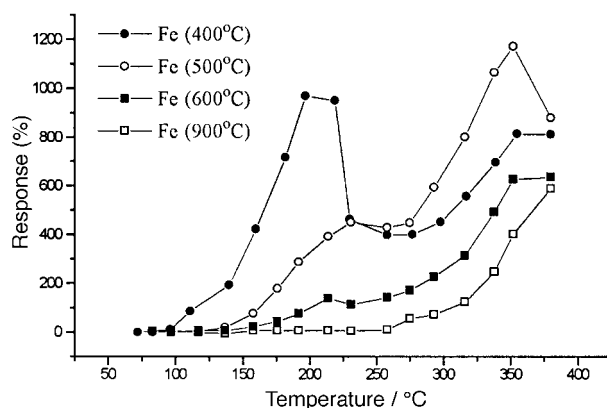


**Fig. 10** Change in temperature profile of sensitivity to 800 ppm CO in dry air for the nominal 5 mol%  $\text{Fe}^{3+}$  doped  $\text{SnO}_2$  sensor as a function of annealing temperature. The samples were prepared by subjecting portions of the same batch of  $\text{Fe}^{3+}$  doped  $\text{SnO}_2$  to 1 h anneals at different temperatures. The data were obtained by subjecting the sensors to 120 s cycles of air/gas/air at each of the available operating temperatures.

to the CO is observed. For this reason, a more limited range of annealing temperatures was considered and detailed calibrations were difficult to perform.

#### Response of surface doped $\text{SnO}_2$ to CO

To further test the hypothesis that the dopants were relocating to surface sites on annealing, deliberately surface doped materials were prepared and their response to the same concentration of CO examined. Samples were prepared surface doped with nominal 1 and 5 mol%  $\text{Cu}^{2+}$  and  $\text{Fe}^{3+}$  cations using the technique previously described. No difference in response to CO was observed between the two dopant concentrations for either of the materials. It should be noted that the technique employed to surface dope the materials is limited in that not all of the  $\text{Cu}^{2+}$  and  $\text{Fe}^{3+}$  ions from the aqueous solutions are deposited onto the surface of the oxide and so the true doping levels are likely to be considerably less than 1 and 5 mol%. Fig. 11 shows the temperature profiles of sensitivity for both the nominal 5 mol%  $\text{Cu}^{2+}$  and  $\text{Fe}^{3+}$  surface doped  $\text{SnO}_2$  in 800 ppm CO in dry air. Both profiles are essentially the same and do not show the characteristic peak in sensitivity at about 200 °C. Only the surface  $\text{Cu}^{2+}$  doped sample shows a slight shoulder at this temperature and clearly direct application of the dopant to the surface does not have the same effect as a more conventional doping approach. In fact, the surface doped materials are behaving more like the well annealed doped

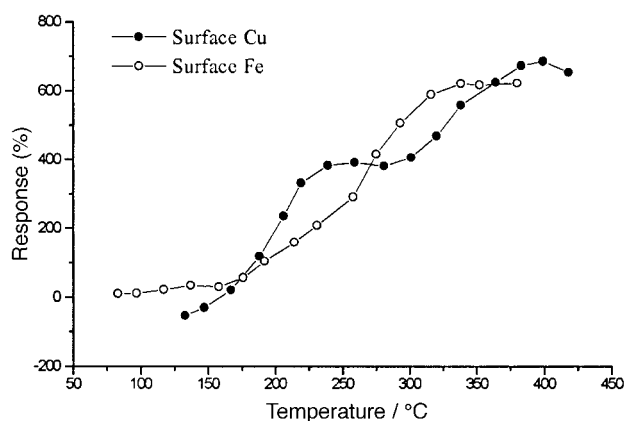


**Fig. 11** Temperature profiles of sensitivity for nominal 5 mol%  $\text{Cu}^{2+}$  (●) and 5 mol%  $\text{Fe}^{3+}$  (○) surface doped  $\text{SnO}_2$  in 800 ppm CO in dry air. The data were obtained by subjecting the sensors to 120 s cycles of air/gas/air at each of the available operating temperatures.

materials. No gain in selectivity is evident from the application of the cation dopants directly to the surface of the SnO<sub>2</sub>. Either the two cations do not show any catalytic activity for the decomposition of CO or their catalytic activity is too small to have any significant effect.

## Discussion

### Response of undoped SnO<sub>2</sub> sensors to CO

Both the undoped and doped sensors exhibit a narrow peak in response to CO at an operating temperature of about 200 °C and at this temperature the response is fast. At temperatures of about 400 °C a considerable response to CO is still obtained but surprisingly the speed of response is much slower. At elevated temperatures, CO is likely to be involved in a combustion reaction with the adsorbed oxygen ions on the surface of the SnO<sub>2</sub>. If this is the case, then the speed of response would be expected to increase with increasing operating temperature as the rate of this combustion reaction increases. The interaction of the CO with the SnO<sub>2</sub> at the two operating temperatures must therefore be by two different mechanisms. At the lower temperature, the CO will be able to permeate into the porous SnO<sub>2</sub> layer and the increased availability of surface catalytic sites as a result of this will lead to a fast response. Conversely, at the higher operating temperature, the CO is likely to combust principally on (or slightly above) the surface and the transfer of electrons liberated by this combustion to the bulk of the oxide will be much slower leading to a reduction in the speed of response.

McAleer *et al.*<sup>25</sup> observed no measurable response to CO in the absence of moisture at operating temperatures below 350 °C but in the presence of moisture, the response was extended over a wider temperature range and peaked at lower temperature. In the present study, the peak in sensitivity at about 200 °C suggests the presence of water. This may be from small amounts of water remaining in the gas stream or may be simply a result of hydroxyl groups on the tin oxide surface. McAleer *et al.*<sup>25</sup> measured the response of a pellet of tin oxide as a function of decreasing temperature from 1000 °C which is sufficient to fully dry the oxide by removing surface hydroxyl groups. When the response of the pellet was measured as a function of increasing temperature they observed a lower peak in sensitivity. The gas sensor test-rig is only able to provide a maximum operating temperature of about 400 °C and at this temperature water desorption will not be complete<sup>2</sup> which is a likely explanation for the low temperature peak in sensitivity.

At the temperature of maximum sensitivity, the magnitude of response was shown to vary linearly with CO concentration when plotted on a ln–ln plot. A common feature of SnO<sub>2</sub> based sensors is that they exhibit a power law conductance response *i.e.* the conductivity is proportional to the concentration of the flammable gas to some power. For CO, it is generally found that the value of the exponential power,  $\beta$ , varies between 0.3 and 0.8, typically 0.5 for pure SnO<sub>2</sub> sensors.<sup>2</sup> The value of  $\beta$  derived from Fig. 4 for the undoped SnO<sub>2</sub> at an operating temperature close to 200 °C is 0.72 which is consistent with this. The detailed origin of the different values of  $\beta$  measured in different studies is not yet clear, although the present work suggests that it is related to differences in crystallite size and fabrication treatment.

The response to CO was shown to be reduced for sensors fabricated from undoped SnO<sub>2</sub> annealed to 900 °C for 1 h. This observation can be attributed to the increased average crystallite size which was determined by XRPD to be of the order of 200 nm at 900 °C compared with about 10 nm at 400 °C and the corresponding reduction in surface area of the material. This is consistent with previous studies.<sup>4,5</sup> Note however that the reduction in sensitivity, even at 200 °C, is by a factor of just over two, whereas the surface area is reduced

by a factor of 20. This suggests that although annealing increases the crystallite size, the larger crystallites are still very porous so that the accessible surface area is still quite large even after annealing. The greatest reduction in response is seen at an operating temperature of about 200 °C (the peak in response), the reduction at 400 °C being much less. This suggests that the response at these two temperatures is *via* different mechanisms as previously discussed.

### Response of Cu<sup>2+</sup> and Fe<sup>3+</sup> doped SnO<sub>2</sub> sensor materials to CO

The temperature profiles of sensitivity for the Cu<sup>2+</sup> and Fe<sup>3+</sup> doped SnO<sub>2</sub> sensors to CO are the same as the undoped SnO<sub>2</sub> profile, *i.e.* peaking in sensitivity at about 200 °C. The effect of doping will be to introduce energy levels within the SnO<sub>2</sub> band gap modifying the conductance.<sup>26</sup> Differences in conductance were evident for materials containing differently charged dopants but the lack of change in the shape of the temperature profile suggests the response mechanism to be the same as for the undoped materials. There is no evidence of the Cu<sup>2+</sup> or Fe<sup>3+</sup> dopants showing increased or different catalytic activity (from that of the SnO<sub>2</sub> surface) towards the combustion of CO. The sensor materials in this study are all prepared at room temperature but are operated at temperatures up to 400 °C and many other fabrication methods of tin oxide based sensors still involve high temperature annealing. For this reason, the stability of any added cationic dopants is an important requirement since any migration could lead to irreproducibility and ageing of the sensor materials. Cu and Fe K-edge EXAFS show the dopant ions to be most likely located on Sn<sup>4+</sup> sites in the lattice in the as-prepared materials.<sup>21</sup> Evidence for this assertion is the detailed fitting of the EXAFS data for these samples and the comparison with the EXAFS of surface doped samples. This is in agreement with computational calculations for +2 and +3 charged dopant ions.<sup>27</sup> The magnitude of the response of these two doped sensors to CO is typically less than that of the undoped material although caution has to be exercised when comparing responses of different sensors due to the dependence of sensitivity on the conductance. The magnitude of response to CO as a function of average crystallite size was investigated by subjecting the doped samples to 1 h anneals at different temperatures. As for the undoped material, the response to CO is seen to decrease as the average crystallite size increases. However, the reduction in response is much greater than for the undoped material with both the Cu<sup>2+</sup> and Fe<sup>3+</sup> doped materials producing almost no response to CO after annealing at 900 °C. The response of the Fe<sup>3+</sup> doped material is shown to decrease more rapidly than the Cu<sup>2+</sup> doped material. The Fe K-edge EXAFS measurements<sup>21</sup> of a nominal 10 mol% Fe<sup>3+</sup> doped SnO<sub>2</sub> sample showed that at 900 °C the dopant precipitated out of the lattice and a separate iron oxide phase formed. This did not occur with the nominal 10 mol% Cu<sup>2+</sup> doped sample indicating the solubility of Fe<sup>3+</sup> to be lower than Cu<sup>2+</sup> in SnO<sub>2</sub> and is a likely explanation for the greater reduction in response to CO described above. Xu *et al.*<sup>5</sup> observed no response from either copper or iron doped SnO<sub>2</sub> sensors and this can most likely be explained by the preparation method they employed which involved the materials all being annealed at temperatures above 600 °C. The greater reduction in response to CO than was observed for the undoped material can only be attributed to the dopant ions. Our EXAFS study<sup>21</sup> showed these dopant ions to be moving as the crystallites are growing, most likely to the surface regions. This relocation of the dopants to the surface must in some way interfere with the gas sensing mechanism although how this occurs is not known. Speculative explanations may be that the dopant ions block the active catalytic sites, perhaps by blocking diffusion channels into the bulk, or that electronic

transfer from the adsorbed gases occurs directly with the dopant ions and not the SnO<sub>2</sub>. This has serious implications in the use of doped SnO<sub>2</sub> materials as gas sensors where elevated temperatures are required. The use of dopants to control the crystallite size is one way in which greater sensitivity is reported to be achieved<sup>4,5</sup> but our results here and in ref. 21 show that the size cannot be the only consideration. Although the growth of the SnO<sub>2</sub> crystallites is impeded by the addition of Cu<sup>2+</sup> and Fe<sup>3+</sup> cations, the response to CO is reduced as the crystallites grow and the dopant ions migrate to the surface regions of the crystallites. Further evidence of this migration being to the surface regions is provided by the comparison of the response to CO of the deliberately surface doped samples (Fig. 11) with those doped samples annealed at 900 °C (Fig. 7). In both cases, the peak in response at ca. 200 °C is absent. It is interesting to note that the response to CO at ca. 400 °C is not so greatly affected and only shows a slight decrease as the materials are annealed. The same is true for the undoped material. This reduction in response can be attributed to the increase in average crystallite size. The migration of the dopants to the surface does not seem to have a large effect on the response of sensors operating at 400 °C and this supports the view that the response at 200 °C is *via* a different mechanism to that at 400 °C. This is further highlighted by the calibration plots for the Cu<sup>2+</sup> doped materials (Fig. 8 and 9). At the lower operating temperature, the calibration lines are not parallel for the 400 and 900 °C annealed doped materials (Fig. 8) whereas they are at the higher operating temperature (Fig. 9). The presence of the dopant in the surface regions affects the response mechanism at the lower operating temperature where the CO is presumably able to penetrate into the porous SnO<sub>2</sub> layer. A possible explanation, although speculative, is that the CO directly interacts with the dopants, *i.e.* electronic transfers occur between CO and the dopant cations and this may be the dominant mechanism at this operating temperature. At the higher operating temperature, the dopant does not appear to influence the mechanism of the CO interaction, although the reasons for this are not known.

Many questions remained unresolved by this present study, namely the mechanisms by which the dopants migrate and the mechanisms by which they interfere with the gas sensing properties once they are at the surface of the tin oxide crystallites. It is our philosophy that improvements can only be made to metal oxide gas sensors by gaining an understanding of their operation by detailed characterisation studies and much more work is needed to further elucidate the mechanisms involved.

## Conclusions

This work has shown how the increases in average crystallite size upon annealing of both pure and metal cation doped SnO<sub>2</sub> sensors results in a reduction in response of these sensors to carbon monoxide. The addition of Cu<sup>2+</sup> and Fe<sup>3+</sup> metal cation dopants both impede the extent of the crystallite growth. However, at temperatures above about 400 °C, both of these dopants begin to migrate from an ordered lattice SnO<sub>2</sub> site to a more disordered region.<sup>21</sup> All of the evidence available suggests these disordered regions to be the surface regions.<sup>21</sup> Any impurity migration can lead to irreproducibility and ageing of the sensors and is therefore an important consideration. This dopant migration has been shown in this study to severely interfere with the response of the doped sensor materials to carbon monoxide. Further studies are required to determine the exact nature of this interference, but it is apparent

that controlling crystallite size by the addition of cation dopants to achieve high sensitivity cannot be the only consideration if the sensor materials are to be operated at elevated temperatures.

We wish to thank the EPSRC and CLRC for providing support for the use of the Daresbury facilities. An award of a CASE studentship by the Health and Safety Laboratory HSL (Sheffield) and EPSRC to S.R.D. is gratefully acknowledged. We would like to thank Dr. S.C. Thorpe at HSL for both his continued interest and support of the sensors research programmes at Kent and his advice with this present study. We also thank Dr. A. Wilson at the University of Birmingham for construction of the gas sensor test-rig and performing preliminary gas sensing studies on the tin oxide materials.

## References

- 1 V. Lantto, in *Gas Sensors; Principles, Operations and Developments*, ed. G. Sberveglieri, Kluwer, Dordrecht, 1992, p. 117.
- 2 D.E. Williams, in *Solid State Gas Sensors*, ed. P. T. Moseley and B. C. Tofield, Adam Hilger, Bristol, 1987, p. 71.
- 3 N. Taguchi, *UK Pat.*, 1280809, 1970.
- 4 C. Xu, J. Tamaki, N. Miura and N. Yamazoe, *Chem. Lett.*, 1990, 441.
- 5 C. Xu, J. Tamaki, N. Miura and N. Yamazoe, *Sens. Actuators B*, 1991, **3**, 147.
- 6 S. R. Davis, A. Wilson and J. D. Wright, *IEE Proc., Circuits, Devices Systems*, in press.
- 7 See for example, G. B. Barbi, J. P. Santos, P. Serrini, P. N. Gibson, M. C. Horrillo and L. Manes, *Sens. Actuators B*, 1995, **25**, 559.
- 8 See for example, M. I. Ivanovskaya, P. A. Bogdanov, D. R. Orlick, A. Gurlo and V. V. Romanovskaya, *Thin Solid Films*, 1997, **296**, 41.
- 9 S. R. Davis, Characterisation of Nanocrystalline Tin Oxide Sensor Materials, Ph.D. Thesis, University of Kent, 1997.
- 10 G. S. Henshaw, V. Dusastre and D. E. Williams, *J. Mater. Chem.*, 1996, **6**, 1351.
- 11 G. S. Henshaw, L. Morris, L. J. Gellman and D. E. Williams, *J. Mater. Chem.*, 1996, **6**, 1883.
- 12 D. Kohl, Oxidic Semiconductor Gas Sensors, in *Gas Sensors; Principles, Operation and Developments*, ed. G. Sberveglieri, Kluwer, Dordrecht, 1992.
- 13 V. N. Mishra and R. P. Agarwal, *Sens. Actuators B*, 1994, **22**, 121.
- 14 J. P. Chatelon, C. Terrier, E. Bernstein, R. Berjoan and J. A. Roger, *Thin Solid Films*, 1994, **247**, 162.
- 15 S. G. Ansari, P. Borojerdian, S. K. Kulkarni, S. R. Sainkar, R. N. Karekar and R. C. Aiyer, *J. Mater. Sci.—Mater. Electron.*, 1996, **7**, 267.
- 16 V. Demarne and R. Sanjines, in *Gas Sensors; Principles, Operations and Developments*, ed. G. Sberveglieri, Kluwer, Dordrecht, 1992, p. 89.
- 17 G. B. Barbi, J. P. Santos, P. Serrini, P. N. Gibson, M. C. Horrillo and L. Manes, *Sens. Actuators B*, 1995, **25**, 559.
- 18 M. J. Fuller and M. E. Warwick, *J. Catal.*, 1974, **34**, 445.
- 19 M. J. Fuller and M. E. Warwick, *J. Catal.*, 1976, **42**, 418.
- 20 T. Maekawa, J. Tamaki, N. Miura and N. Yamazoe, *J. Mater. Chem.*, 1994, **4**, 1259.
- 21 S. R. Davis, A. V. Chadwick and J. D. Wright, *J. Phys. Chem. B*, 1997, **101**, 9901.
- 22 K. Matar, D. Zhao, D. Goldfarb, W. Azelee, W. Daniel and P. G. Harrison, *J. Phys. Chem.*, 1995, **99**, 9966.
- 23 H. P. Klug and L. E. Alexander, *X-Ray Diffraction Procedures*, Wiley, New York, 1974.
- 24 P. B. M. Archer, A. V. Chadwick, J. J. Miasik, M. Tamizi and J. D. Wright, *Sens. Actuators*, 1989, **16**, 379.
- 25 J. F. McAleer, P. T. Moseley, J. O. W. Norris and D. E. Williams, *J. Chem. Soc., Faraday Trans.*, 1987, **83**, 1323.
- 26 P. A. Cox., *The Electronic Structure and Chemistry of Solids*, Oxford University Press, Oxford, 1987.
- 27 C. M. Freeman and C. R. A. Catlow, *J. Solid State Chem.*, 1990, **85**, 65.

Paper 8/03866J; Received 22nd May, 1998